Hindawi
Geofluids
Volume 2023, Article ID 8839852, 16 pages
https://doi.org/10.1155/2023/8839852

Research Article

Effect of Water Content on the Impact Propensity of White Sandstone

Jiankui Bai,[1,2] **Chuanming Li**,[1,2] **Ruimin Feng**,[3] **Nan Liu**,[4] **Xiang Gao**,[1,2] **Zhengrong Zhang**,[1,2] **and Bochao Nie**[1,2]

[1]*School of Mining Engineering, Anhui University of Science and Technology, Huainan 232001, China*
[2]*Key Laboratory of Safety and High-Efficiency Coal Mining, Ministry of Education (Anhui University of Science and Technology), Huainan 232001, China*
[3]*Department of Civil Engineering, University of Arkansas, Fayetteville, AR 72701, USA*
[4]*College of Energy and Mining Engineering, Shandong University of Science and Technology, Qingdao 266590, China*

Correspondence should be addressed to Chuanming Li; chuanmingli@126.com

Received 8 July 2023; Revised 11 September 2023; Accepted 26 September 2023; Published 17 October 2023

Academic Editor: Yi Xue

Impact ground pressure is one of the most common dynamic disasters induced by mining activities, and water content is an important factor affecting such dynamic disasters. In this paper, uniaxial compression test, cyclic loading and unloading test, and acoustic emission test were conducted on white sandstone using RMT-150B rock mechanics test system and DS5 acoustic emission test system. The influence law of water content was analyzed on the strength characteristics, energy change characteristics, and impact propensity of white sandstone. The results showed that (1) the internal structure of the sandstone gets softened with the increase of the water content. The cohesive effect within the rock also begins to weaken, which in turn reduces the stiffness of the material and enhances its plasticity. The ability of the rock to resist elastic deformation becomes weaker, resulting in lower compressive strength and elastic modulus when the rock is subjected to external forces, making it more prone to deform and fail. The decrease in compressive strength of the water-saturated rock is 33.3%, and the decrease in its elastic modulus is 28.1% compared to the dry rock. (2) As the water content increases, the cohesion of the rock decreases and the internal structure of the rock fails more easily, which ultimately makes the energy needed for rock destruction lower. As a result, the total energy, elastic energy, and dissipative energy of the rock are reduced. The accumulated AE energy also decreases with the increase of the water content, indicating that rocks with higher water content gather less elastic energy before damage and accumulate less energy when deformation damage occurs. (3) The impact energy index and elastic energy index are negatively correlated with the water content. The impact energy index is reduced by 28.6%, and the elastic energy index is reduced by 20.9% for the saturated rock compared to the dry rock. The elastic energy index and impact energy index both decrease with the increase of rock water content, indicating that the less elastic energy is stored before the destruction of the rock and no excess energy is transformed into energy in rock crushing when the rock breaks, and therefore, the impact propensity of the rock is smaller. The results of the study can provide a theoretical basis for underground construction as well as rock fracture destabilization.

1. Introduction

Due to the increasing intensity of mining activity and the deeper depth of coal mines in China, dynamic disasters such as impact ground pressure occur more frequently; therefore, the safety of coal production will be seriously threatened. Rock impact propensity is an important indicator of the likelihood of impact ground pressure, which is influenced by the surrounding stress environment as well as the state of the rock itself. The water content of the rock is one of the most critical factors affecting the mechanical properties of the rock and the impact propensity of the rock, and water

injection can be adapted to soften the roof rock, which has become a common prevention and control technical measure. Therefore, it is of great engineering importance to study the effect of water content on the rock impact propensity.

Many scholars have conducted studies on the effects of water content on the deformation characteristics, strength characteristics, and energy evolution patterns of rocks. Zheng et al. [1] conducted uniaxial compression tests on rocks with different water contents and analyzed the relationship between water content and the softening and brittleness coefficients of hard rock materials. Mao et al. [2] conducted uniaxial compression tests on coal rocks with different water contents and obtained the laws of impact propensity of rocks with different water contents. Tao [3] summarized rock burst phenomena around the world and found that rock impact propensity is affected by the degree of rock hardness and reported that acoustic emission phenomena always accompany the process of rock burst occurrence. Su et al. [4] conducted uniaxial tests on coal rocks in different saturated states and concluded that the impact of coal rocks would be reduced after water soaking. Fu [5] conducted uniaxial compression tests and acoustic emission tests on rocks and obtained the correspondence between the sabotage rates of rocks and the number of acoustic emission events. Yang et al. [6] analyzed the characteristics of energy release and dissipation and proposed that the unit time release rate can be used as a basis for judging the impact propensity of rock. Pu et al. [7] conducted triaxial compression tests on rocks under different confining pressures and analyzed the effects of confining pressure on the deformation law of rocks and the energy evolution characteristics. Roy et al. [8] investigated the effect of different water saturation times on the mechanical parameters of sandstone, and the results showed that the saturation of the rock has a negative impact on the tensile strength, Young's modulus, and fracture stiffness. Jansen et al. [9] used acoustic emission technique to study the three-dimensional microcrack distribution during rock damage, which illustrated the damage characteristics and the process of crack extension in rocks.

Previous studies have greatly improved our understanding of the strength change during the destabilization process of water-bearing rocks, but an in-depth investigation is required on the effect of water content on rock strength characteristics, energy characteristics, and rock impact propensity from the perspective of underground coal mining. Uniaxial compression tests and cyclic loading and unloading tests are used to study the mechanical properties of rocks since these tests can be used to simulate cyclic load in real engineering geological environments, thus exploring issues such as the strength characteristics of rocks and the energy evolution mechanism.

Therefore, in this paper, relevant tests were conducted on sandstones with different water contents and also on the influence law of water content on the strength characteristics, energy distribution characteristics, and rock impact propensity. This study can not only provide theoretical basis and reference for the safe construction of coal mine underground and the prevention and control of dynamic disasters but also has important practical significance for analyzing the damage of engineering rock body (such as rock explosion) and the stability of underground engineering surrounding rock.

2. Experimental Work

2.1. Experimental Equipment and Specimen Preparation. The types of experimental equipment we used in this study are RMT-150B rock mechanics test system and DS5 series acoustic emission test system. RMT-150B rock mechanics experimental system can be carried out under computer control, is easy to operate, and has fully functional conditions, while manual intervention can be made during the test to modify the control mode and test steps. DS5 series acoustic emission system adopts USB3.0 interface for data transmission, which can reach up to 48 channels of synchronous data acquisition, and more precise positioning effect can be achieved through more channels of data acquisition.

The rocks were processed into standard specimens with dimensions of 50 × 100 mm by a coring machine and trimmed by a cutting machine [10]. The two ends of each specimen will be polished smoothly and parallel to each other to reduce the experimental error. Figure 1 shows the test equipment as well as the well-prepared sandstone specimens.

2.2. Experimental Protocol and Procedure. After the rock specimens were prepared, they were divided into 3 groups: dry state, natural state, and saturated state. The average water content of white sandstone in its natural state is 0.18%. In order to minimize the errors induced by the difference of the sandstone specimens in the dry state and saturated state, the weight of the samples was measured regularly until the weighed mass of the sandstone specimens remained constant.

In the experimental process, the sandstone rock samples of the natural group were not treated; then, the remaining six rock samples were put into the oven at 100°C for constant temperature drying for 48 h, taken out, and put into the drying oven to cool down to room temperature. When the weight change did not exceed 0.05%, the rock samples were considered to be completely dried, and three rock samples were selected as the drying group [11]. The specimen preparation of the saturated group selected three dried rock samples using the natural water immersion method for its water absorption treatment. The specimens were removed at regular intervals, and the surface water was wiped off with a towel and weighed until the moisture content of the rock samples stabilized.

As shown in Table 1, the average moisture content was finally obtained from the test: 0.18% for the natural group, 2.19% for the saturated group, and 0% for the dry group.

As shown in Figure 1(a), a standard rock specimen was placed on the RMT loading table, acoustic emission probes were pasted on both sides of the rock specimen, and the data were monitored in real time by the acoustic emission system. DS5 series acoustic emission test system is equipped with a probe to collect signals, the preamplification gain is 40 dB,

(a) Pictures of the operating system

(b) Rock mechanics test system

(c) White sandstone specimens

Figure 1: Experimental system and white sandstone specimen diagram.

Table 1: Water content of rocks in different states.

Rock sample state	Rock sample number	Dry weights (g)	Wet weight (g)	Water content (%)	Average moisture content (%)
Dry state	1-1	461.34			0
	1-2	458.95			
	1-3	460.77			
Natural state	2-1	469.99	470.73	0.15	0.18
	2-2	471.85	472.77	0.19	
	2-3	469.65	470.57	0.20	
Saturation state	3-1	474.36	484.98	2.24	2.19
	3-2	472.63	483.54	2.31	
	3-3	473.98	483.89	2.01	

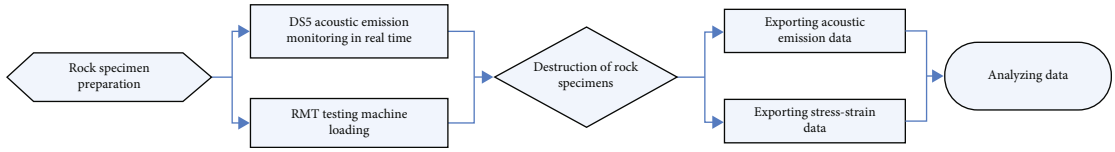

Figure 2: A flowchart showing the experimental procedures and data that need to be recorded.

the threshold is set to 50 dB, and the sampling rate is set to 2.5 MHz. The loading process of the testing machine is controlled by the RMT operating system until the rock specimen is completely destroyed and the test is completed. Additionally, Figure 2 shows a flowchart which specifies the experimental data that need to be recorded during the tests.

2.2.1. Uniaxial Compression Test. After the rock specimens were prepared, they were divided into 3 groups for uniaxial compression test; each group included 3 pieces of dry state rock specimens, 3 pieces of natural state rock specimens, and 3 pieces of saturated state rock specimens. Uniaxial compression tests were conducted to determine the changes in the strength and elastic modulus of sandstone specimens with different water contents and then to analyze the relationship between the energy evolution pattern of the rock and the water content throughout the process.

2.2.2. Cyclic Loading and Unloading Test. In addition, three groups of rock samples have been selected for cyclic loading and unloading tests. The parameters of cyclic energy aggregation, release, and dissipation at all levels are obtained by cyclic loading and unloading tests, and the rock strength characteristics are analyzed. The RMT-150B rock mechanics system uses ramp wave control force for graded loading and unloading, and the test loading and unloading rate is 0.5 KN/s. To facilitate later data analysis, the force interval is $0 \rightarrow 5 \rightarrow 0 \rightarrow 10...$, each interval is cycled once, and this cycle continues until the rock sample fails.

The acoustic emission probe was tightly attached to the side surface of the rock using coupling agent before the test for ensuring the effectiveness and accuracy of the acoustic emission signal.

During the whole experiment, the rock mechanics test system and the acoustic emission test system need to be operated simultaneously. The rock mechanics test system automatically collects stress and strain against time and draws stress-strain curve and displacement-load curve; and the acoustic emission system automatically collects ringing count, energy, amplitude, and other parameters.

3. Effect of Water Content on Rock Mechanical Properties

The compressive strength of rocks with different water-bearing states was calculated from the results of the three groups of rocks, and the relationship curves of compressive strength of rocks with different water-bearing states were plotted based on the average values of compressive strength and elastic modulus.

When a rock specimen contains water, the internal skeleton of the rock deforms under external loads, causing the pore space to compress or stretch. Due to the incompressibility of water, when the pore space is smaller than the volume of water (mainly free water) within the pore space, it results in water starting to flow under external loads. The squeezing of water inside the rock leads not only to higher pore water pressure but also to outward tensile stresses inside the rock. As a result, tensile stress concentration occurs at the pore ends, which in turn exacerbates crack extension [12]. The attenuation of the compressive strength of rocks after water absorption responds to the softening effect of water on their structure. Therefore, the concept of "softening factor" was introduced [13]. The softening coefficient reflects the change in mechanical strength of the rock before and after water absorption, reflecting the engineering geological properties of the rock. The formula is as follows:

$$K_{(C/T)} = \frac{\sigma_s}{\sigma_d}, \tag{1}$$

where K_C and K_T are the compressive and tensile softening coefficients of the rock, respectively; σ_d is the compressive/tensile strength of the dry specimen (MPa); and σ_s is the compressive/tensile strength of the specimen in different water content states (MPa).

Based on the resultant parameters in Table 2, the compressive softening coefficients K_C of the rocks in different water-bearing states can be calculated separately. As can be seen in Figure 3, under uniaxial compression and cyclic loading and unloading conditions, a higher water content leads to a smaller rock compressive softening coefficient.

The testing results in Figures 3 and 4 show that the water content of the rock negatively impacts its internal structure. The cohesive effect within the rock begins to weaken with the increase of the water content, which thus reduces the stiffness of the material and increases the plasticity. The ability of the rock to resist elastic deformation is weaker, resulting in lower compressive strength and elastic modulus when the rock is subjected to external forces; hence, the rock is more prone to deform and fail.

Due to the different test conditions, the compressive strength and elastic modulus parameters obtained by cyclic loading and unloading tests for rocks with the same water-bearing state are reduced compared to those obtained under uniaxial compression conditions, and the decreases in compressive strength and elastic modulus for rocks with cyclic loading and unloading tests compared to uniaxial compression tests for the three water-bearing states are 31.8%, 44.2%, and 28.2%, respectively; the decreases in elastic modulus are 6.4%, 15.9%, and 17.8%, respectively. The reason for

Table 2: Parameters of test results.

Experimental conditions	Rock water content status	Average modulus of elasticity (GPa)	Average compressive strength (MPa)
Uniaxial compression	Dry state	8.109	56.448
	Natural state	8.084	53.554
	Saturated state	5.832	35.781
Cyclic loading and unloading	Dry state	7.589	38.486
	Natural state	6.251	29.885
	Saturated state	4.792	25.658

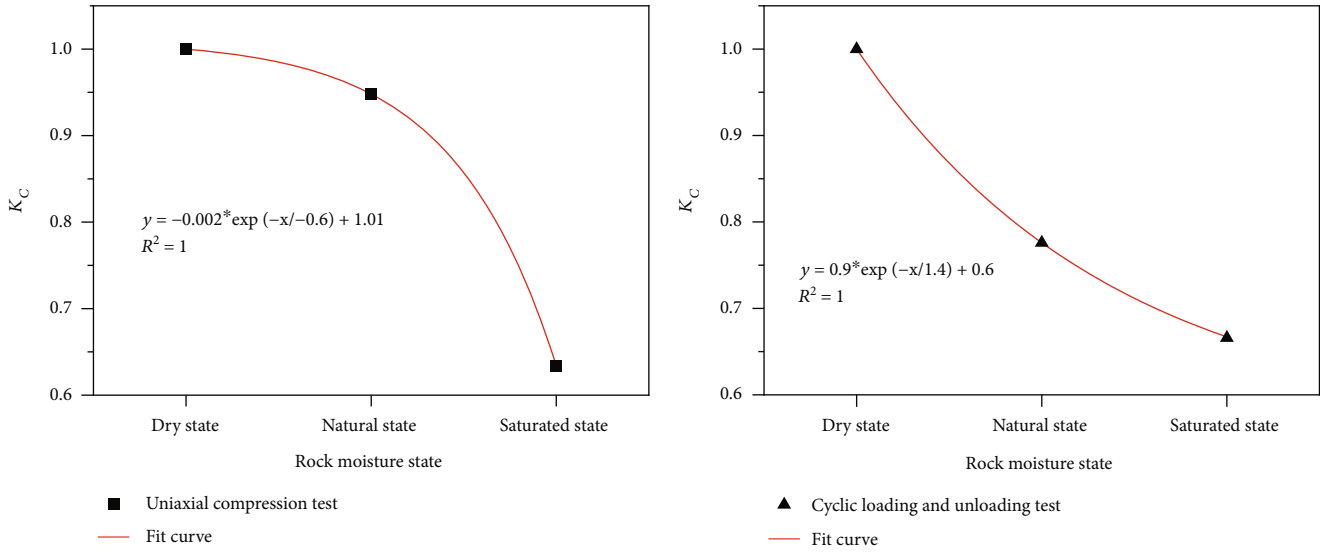

(a) Uniaxial compression test

(b) Cyclic loading and unloading test

Figure 3: Relationship between the coefficient of compressive softening of rocks and the state of water content.

this can be attributed to energy loss during loading and unloading before the peak rock strength is reached in the cyclic loading and unloading test.

4. Effect of Water Content on the Energy Characteristics of Rocks

4.1. Uniaxial Compression Test Energy Analysis. It is considered that a unit volume of rock unit is deformed under the action of external forces, assuming that there is no heat exchange between the physical process and the outside world, and the total input energy generated by external work is U. According to the first law of thermodynamics, the following equation can be obtained:

$$U = U^{d} + U^{e}, \tag{2}$$

where U^{d} is the unit dissipation energy and U^{e} is the unit releasable elastic strain energy.

Figure 5 shows the stress-strain curve of the rock unit. The area U_i^{d} indicates the energy consumed when the unit undergoes damage and plastic deformation, and the shaded area U_i^{e} indicates the releasable strain energy stored in the unit, which is the elastic strain energy released after the unloading of the rock unit.

Assuming that there is no heat exchange between the system and the outside world during the test, the energy U generated by the external work is the actual energy U_0 absorbed by the rock sample. Under uniaxial compression conditions,

$$U_0 = \int \sigma_1 d\varepsilon_1 = \sum_{i=0}^{n} \frac{1}{2}(\varepsilon_{1i+1} - \varepsilon_{1i})(\sigma_{1i} + \sigma_{1i+1}), \tag{3}$$

$$U^{e} = \frac{1}{2}\sigma_1 \varepsilon_1^{e} = \frac{\sigma_1^2}{2E_u} \approx \frac{\sigma_1^2}{2E_0}, \tag{4}$$

where σ_{1i} and ε_{1i} are the stress and strain values at each point on the stress-strain curve, respectively, and E_u is the modulus of elasticity of unloading, and the initial modulus of elasticity E_0 is taken instead of E_u in the calculation [14]. The value of E_0 is taken as 50-60% of the peak strength of the elastic phase of the rock.

Based on the results obtained from uniaxial compression tests of rocks with different water contents, the stress-strain energy variation curves of rocks with different water-bearing states are plotted in Figure 6.

The uniaxial compression curve of the rock includes compaction phase, elastic phase, plastic phase, and damage phase. It can be inferred from the figure that the fractures

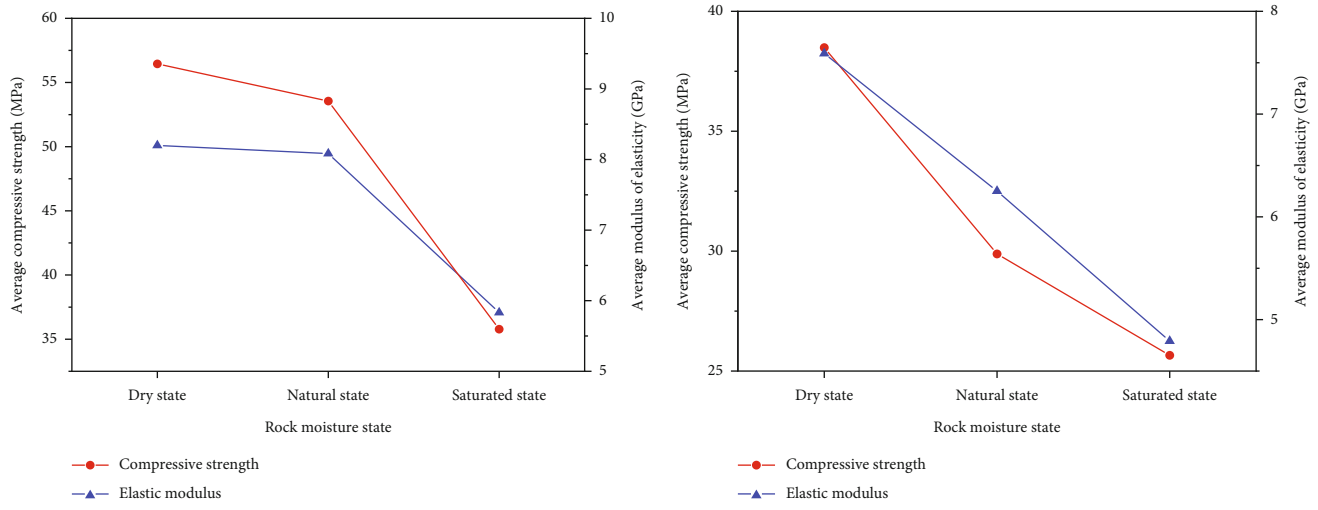

(a) Uniaxial compression test

(b) Cyclic loading and unloading test

Figure 4: Relationship between water content and compressive strength and modulus of elasticity of rocks.

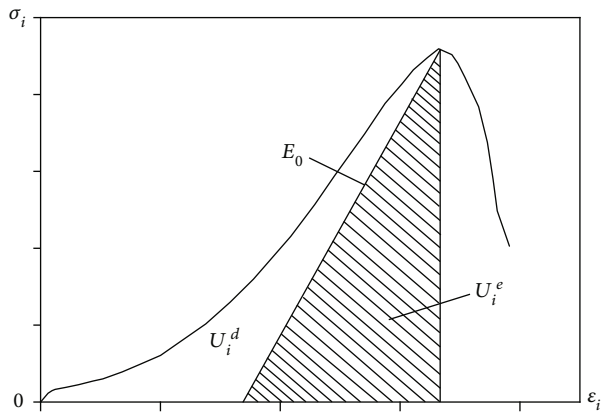

Figure 5: Quantitative relationship between energy dissipation U_i^{d} and releasable strain energy U_i^{e} in unit volume.

inside the rock will gradually close under the action of external forces during the compaction phase and the elastic phase, when the total energy absorbed by the rock is all stored inside the rock in the form of elastic energy, and almost no dissipative energy is generated during these two phases. In the plastic stage, the internal cracks in the rock are gradually expanding by external forces, and the internal structural changes become complicated. The rate of increase of elastic energy becomes slower at this stage, the dissipation energy gradually starts to increase, and the internal damage of the rock further intensifies. When the peak rock strength is reached, the elastic energy is released rapidly and the dissipation energy increases sharply. The bearing capacity of the rock is rapidly reduced after damage, and a certain residual strength is maintained. In this period, the energy absorbed by the rock is basically converted into dissipated energy, which is used for further development of rock fracture and shear deformation of the sliding plane. The intersection of the elastic energy curve and the dissipative energy curve is called "energy dividing point," before which the energy accumulation is mainly manifested and after which the energy dissipation is mainly manifested.

The acoustic emission energy collected by the DS5 acoustic emission test system is the remaining elastic energy measured from the material surface after propagation attenuation, that is, the elastic energy released by the acoustic emission source. According to the experimental results, it can be seen that the cumulative AE energy increases gradually with the increase of strain, and there is a positive correlation between strain and damage in the deformation process of rock mass. Therefore, cumulative AE energy must also have some connection to damage. Liu and Wang [15] obtained the relationship between strain and cumulative AE energy by conducting various tests and derived the theoretical relationship between cumulative AE energy and stress strain, as expressed by

$$W_{\mathrm{S}} = \frac{1}{b}\left\{\ln\frac{1}{a}\left[\frac{1}{n\gamma}\left(\frac{1}{2}E_0\varepsilon^2 + \frac{1}{3}A\varepsilon^3\right)\right]^{n/n-1}\right\}, \tag{5}$$

$$\sigma = \left(E_0\varepsilon + A\varepsilon^2\right)\left\{1 - \left[a\exp\left(bW_{\mathrm{S}}\right)\right]^{1/n}\right\}, \tag{6}$$

where w_s is the cumulative AE energy; a and b are constants; n, A, and E_0 are material constants; γ is the damage energy dissipation rate of the rock material; and ε is strain.

As can be seen from the figure, basically no acoustic emission energy is generated during the rock compaction phase, as no significant structural changes occur within the rock. After entering the elastic phase, the cumulative acoustic emission energy gradually increases. The accumulated AE energy reaches a maximum when the peak rock intensity is reached, the energy after the peak intensity is dominated by dissipative energy, and the elastic energy is rapidly reduced to a minimum, so that the acoustic emission energy is also reduced to a minimum or even disappears.

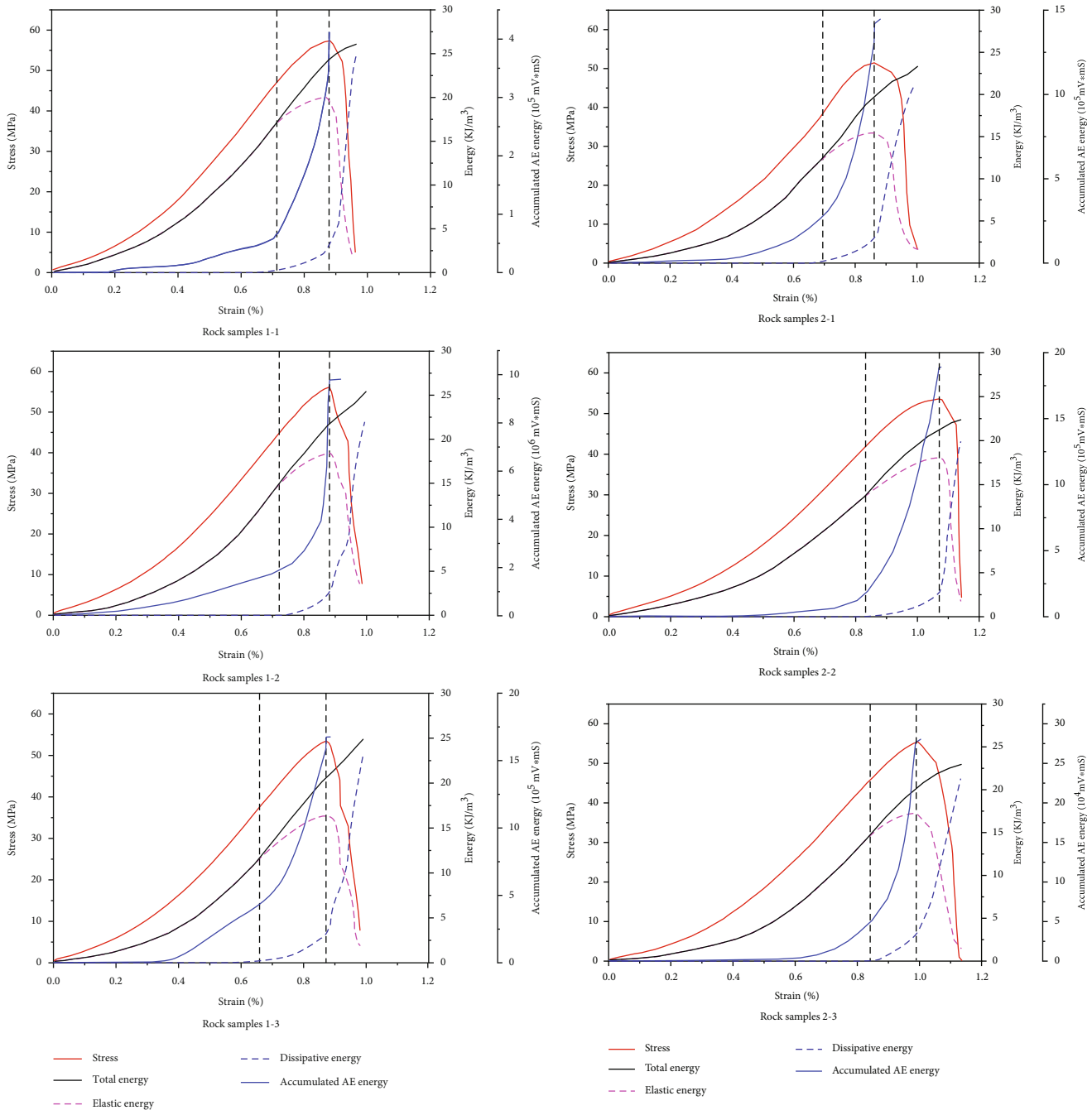

(a) Dry state

(b) Natural state

Figure 6: Continued.

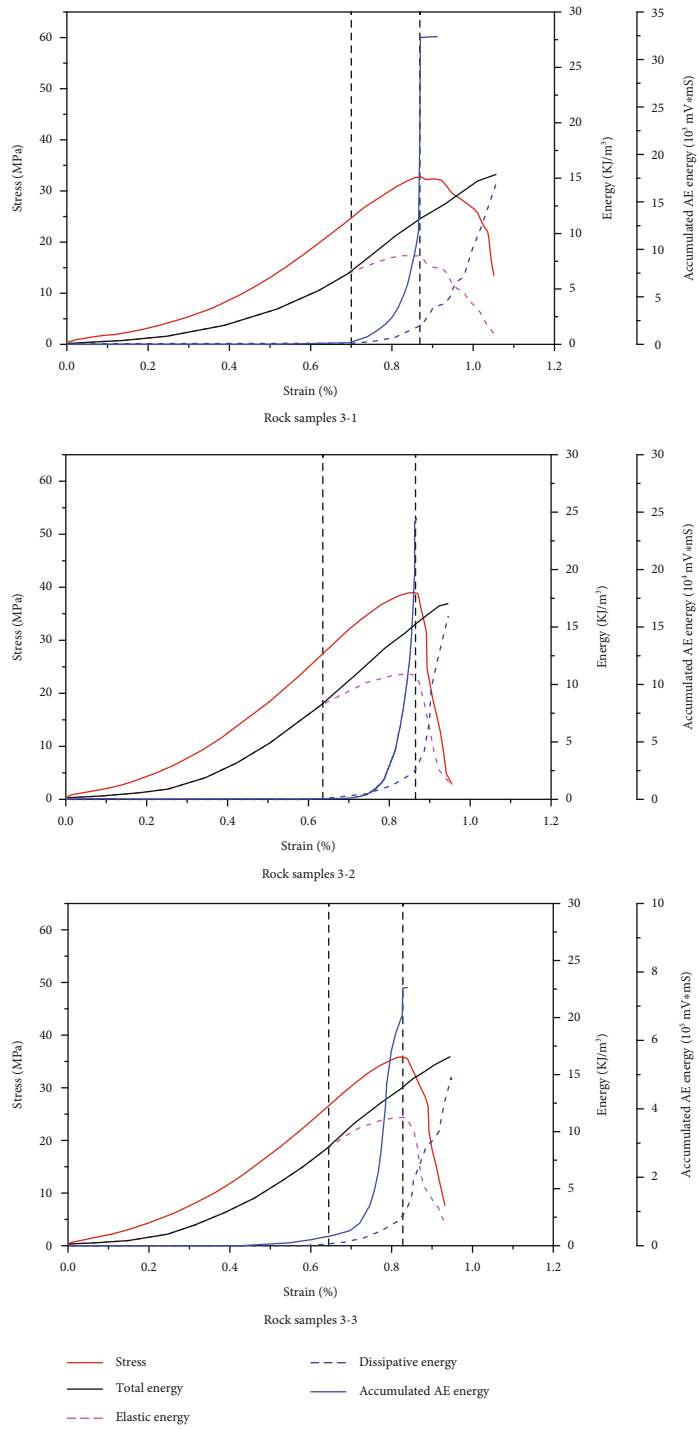

(c) Saturated state

Figure 6: Stress-strain energy variation curves for rocks with different water content states.

According to the stress-strain energy variation curves for rocks with different water content states in Figure 6, the specific changes of total energy, elastic energy, and dissipation energy of rocks in three water-bearing states are compared and analyzed in Figure 7.

From the resulting parameters, the average value of the total energy of the rock can be calculated: 25.46 kJ/m^3 in the dry state, 22.88 kJ/m^3 in the natural state, and 16.31 kJ/m^3 in the saturated state. In Figure 7(a), with the increase of the water content, the total energy absorbed decreases subsequently, which is consistent with the trend of the compressive strength of the rock versus water content. As shown in Figure 7(c), since the total energy decreases with the increase of water content, the elastic energy and dissipation energy also show a decreasing trend. After the dramatic energy change, the percentage of elastic energy in the total

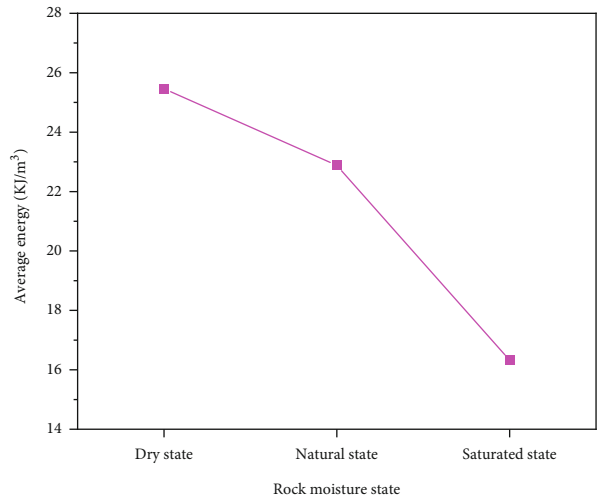

(a) Relationship between water content and total energy

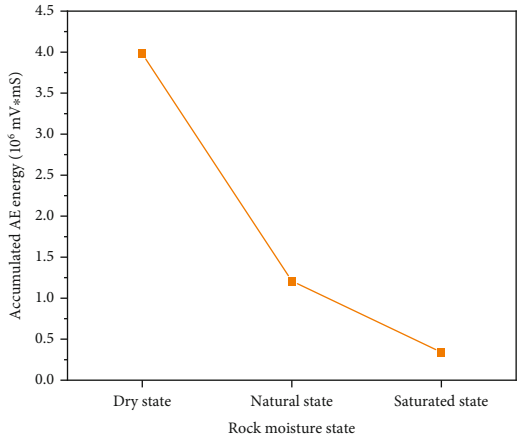

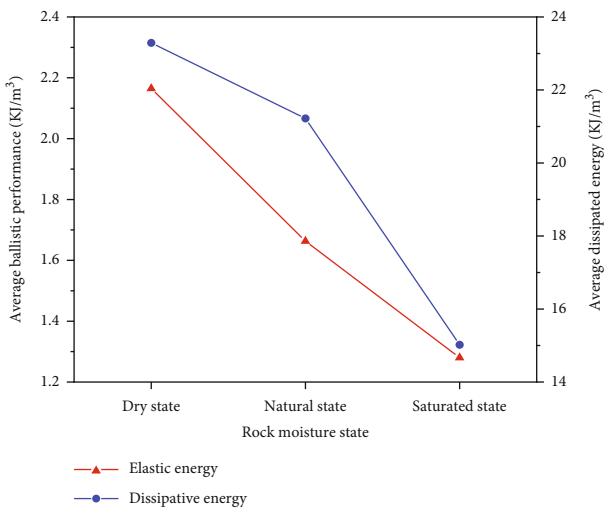

(b) Relationship between water content and accumulated AE energy (c) Relationship between water content and elastic energy and dissipation energy

Figure 7: Relationship between water content and each energy change.

energy gradually decreases, while the percentage of dissipative energy in the total energy gradually increases. The accumulated AE energy decreases from 3.98×10^6 mV∗mS to 0.34×10^6 mV∗mS, which laterally reflects that the elastic energy inside the rock shows a decreasing trend with the increase of water content.

4.2. Energy Analysis of Cyclic Loading and Unloading Tests. The cyclic loading and unloading stress-strain curves are shown in Figure 8, where the area enclosed by the loading curve OA and the strain ε (OAB) is the total energy absorbed by the rock U_0 [16]; the area enclosed by the unloading curve AC and the strain ε (ABC) is the elastic energy U^e accumulated inside the rock; and the area enclosed by the loading curve, the unloading curve, and the strain ε (OAC) is the dissipation energy U^d of the rock.

The loading and unloading curves intersect during the graded loading and unloading process to form a closed hysteresis loop area. The hysteresis loop area (CDC) represents the hysteresis effect energy U^{ed} during uniaxial compression. Since the hysteresis effect energy exists during the loading and unloading of the rock, a part of the unloading hysteresis effect energy can be stored inside the rock before the rock is unloaded, but this part of the hysteresis effect energy is not reversible, so the hysteresis effect energy belongs to the special dissipation energy, which can be stored inside the rock and is not reversible [17]. Based on the above analysis, the dissipation energy of the rock (area enclosed by OAC) can be divided into hysteresis effect energy (area enclosed by CDC) U^{ed} and plastic dissipation energy (area enclosed by OADC) U^{dd}.

Equations of elastic energy and dissipation energy are mathematically expressed as follows:

$$U^e = \int_0^{\varepsilon_1} \sigma_i d\varepsilon_i, \tag{7}$$

$$U^d = \int_0^{\varepsilon_1} \sigma_i d\varepsilon_i - \int_{\varepsilon_2}^{\varepsilon_1} \sigma_i d\varepsilon_i, \tag{8}$$

where ε_1 is the corresponding strain value at σ_1, σ_1 is the stress value at any point on the stress-strain curve, ε_2 is the strain value at the unloading stage where the stress is 0, and ε_1 is the stress value and strain value of σ_1 for the i^{th} cycle, respectively.

Based on the results obtained from cyclic loading and unloading tests of rocks with different water contents, the stress-strain energy variation curves of rocks with different water-bearing states are plotted in Figure 9.

The total energy in the cyclic loading and unloading process is also composed of elastic and dissipative energy. Starting from the first stage of the cycle, the elastic energy and dissipation energy gradually increase, and both increase with the number of cycle stages. The elastic energy reaches its maximum when a critical state of dramatic energy change is reached, after which it shows a sharp downward trend. The dissipative energy increases sharply after a dramatic change in energy until it reaches a maximum value when the rock is completely deformed and destroyed, while the elastic energy decreases to a minimum or even disappears.

In the process of chemical erosion damage of rocks, water will reduce the cohesive energy and cohesion of rocks and destroy the internal mechanical structure of rocks. From the energy point of view, the strength and modulus of elasticity of rocks in the water-bearing state declined and plastic deformation increased, leading to an increase in the dissipated energy and a decrease in the energy storage of rocks during the loading process [16].

With the increase of water content, the time of elastic deformation stage and yield stage of rock during compression will be shortened. This is because the internal friction force of the rock decreases after it is hydrated, the resistance to deformation gradually decreases, and the fracture area inside the rock becomes larger, which can reach the strain required for yield and damage faster [18]. Thus, rocks with high water content absorb less elastic energy during the elastic deformation phase. In Figure 9, it can be seen that the total energy (OAB) and the area of the hysteresis loop (CDC) of the saturated state rock are the largest at the same number of cyclic stages, which indicates that the presence of water increases the percentage of dissipated energy during cyclic loading and unloading of the rock. The dissipation of energy is mainly used for the germination and expansion of cracks within the rock. Therefore, rocks with high water content are more likely to reach a state of destruction and require lower energy.

Based on the resulting parameters, the average total energy of the rock can be obtained: 22.32 kJ/m^3 in the dry state, 16.32 kJ/m^3 in the natural state, and 15.08 kJ/m^3 in the saturated state. In Figure 10(a), the higher water content of the rock leads to the less total energy being absorbed. In Figure 10(c), the total energy, elastic energy, and dissipation energy of the rock decrease with the increase of water content. After the dramatic energy change, the percentage of elastic energy in the total energy gradually decreases, while the percentage of dissipative energy in the total energy gradually increases.

The accumulated AE energy increases slowly during the first cyclic loading and unloading interval, and with the increase of axial stress, the accumulated AE energy curve rises in the form of a step, and the obvious stage of the rise

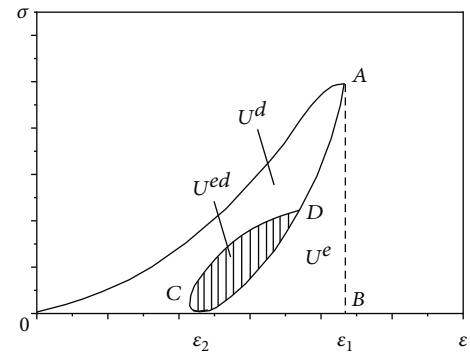

Figure 8: Cyclic loading and unloading energy diagram.

indicates that the acoustic emission activity is more active, mainly concentrated in the process of loading and unloading. Relatively stabilise acoustic emission activity when in the interval between two cycles. At the last stage of loading, the slope of the accumulated AE energy curve of the three states is the largest and the increase is also the largest, indicating that the acoustic emission activity is pretty active at this time, and the crack expansion and complete penetration mainly occur at this stage.

As shown in Figure 9, the dry state rock has a peak accumulated AE energy of 31×105 mV $*$ mS during the 8th stage of the cycle, at which time the rock is damaged at 38.340 MPa. The natural state rock has a peak cumulative AE energy of 0.5×105 mV $*$ mS during the 6th stage of the cycle, at which time the rock is damaged at 30.507 MPa. The peak accumulated AE energy of the saturated state rock is 0.13×105 mV $*$ mS during the 5th stage of the cycle, at which time the rock is damaged at 25.455 MPa. The accumulated AE energy decreased from 31×105 mV $*$ mS to 0.13×105 mV $*$ mS with increasing water content of the rock, with a decrease of 99.6%, which is consistent with the trend of uniaxial compression test. Therefore, the higher the water content of the rock, the smaller the accumulated AE energy, indicating that the higher the water content of the rock, the less elastic energy is gathered, and the lower energy is reached when deformation damage occurs.

Figure 11 shows that the energy parameters of the uniaxial compression test rocks are generally higher than those of the cyclic loading and unloading test rocks for the same water-bearing state. The decrease of elastic energy of the rock in the cyclic loading and unloading test compared with the uniaxial compression test in the three water-bearing states is 3.21%, 35.70%, and 34.06%; the decrease of dissipation energy of the rock is 13.12%, 28.14%, and 5.23%; and the decrease of total energy of the rock is 12.84%, 28.68%, and 7.55%, respectively.

In summary, through the uniaxial compression test and cyclic loading and unloading test, the process of deformation and damage of rock by external forces is the process of energy gathering, energy dissipation, and energy release from the energy perspective. As the water content increases, the cohesion of the rock decreases and the internal structure of the rock

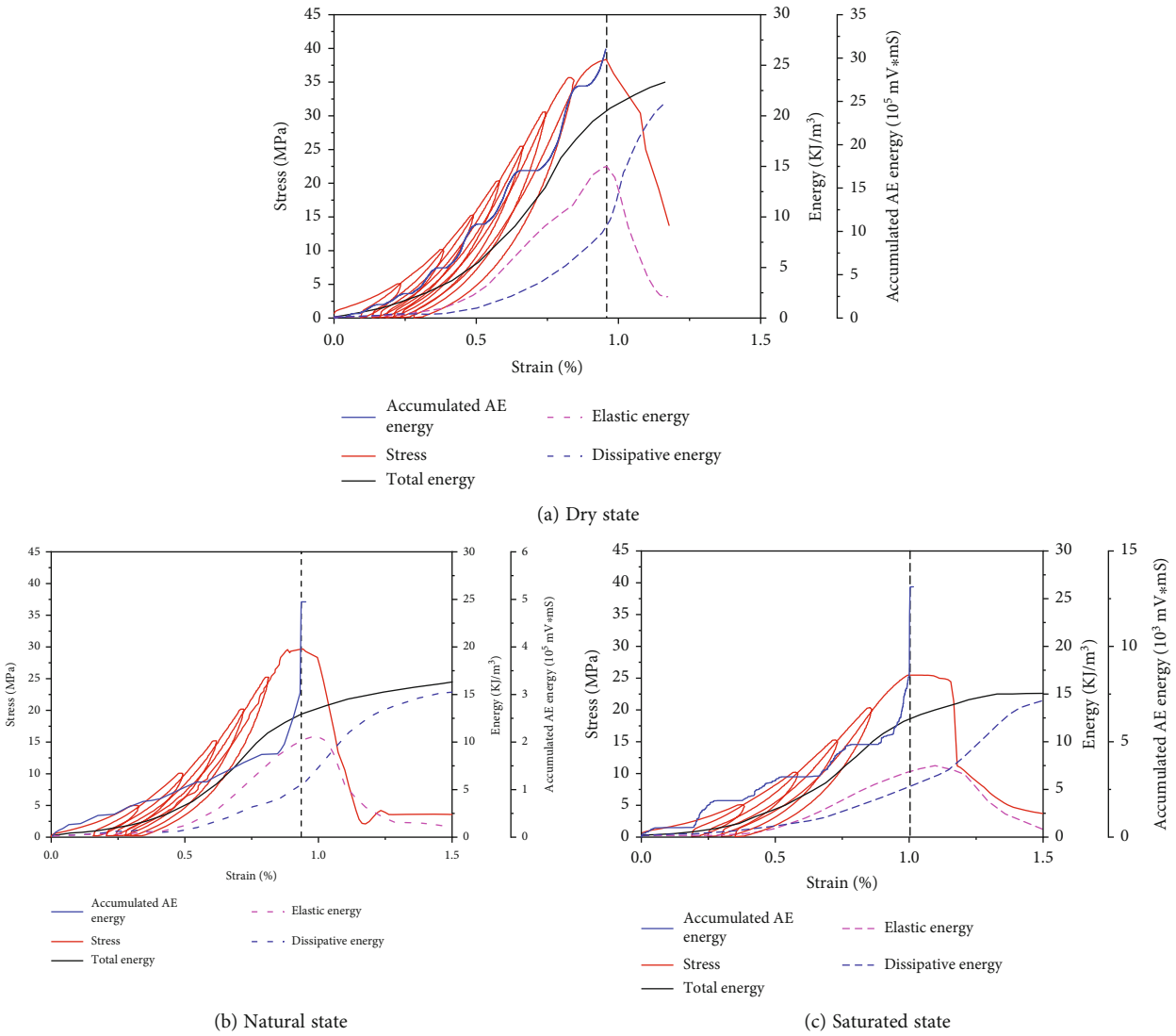

Figure 9: Stress-strain energy variation curves for rocks with different water-bearing states.

is more easily destroyed, which eventually makes the energy reached by the rock decrease. As a result, the total energy absorbed by the rock, the elastic energy, and the dissipated energy are reduced. The accumulated AE energy also decreases with the increase of the water content of the rock, indicating that the higher the water content of the rock, the less elastic energy is gathered before the damage, and the lower energy is reached when the deformation damage occurs.

The same aspects for both are as follows: the less energy absorbed as the water content of the rock increases. The change law of elastic energy and dissipative energy is roughly the same; before the dramatic change in energy, elastic energy accounts for a larger proportion of the total energy, and energy is dominated by elastic energy. After a dramatic change in energy, dissipated energy then accounts for a larger proportion of the total energy, and energy is dominated by dissipated energy. The different aspects are as follows: uniaxial compression tests have a shorter test time and no energy loss before plastic deformation of the rock occurs compared to the cyclic loading and unloading test, so there is no increase in dissipation energy upfront. The dissipative energy only starts to increase gradually after the plastic phase.

4.3. Rock Damage Pattern Analysis. As shown in Figure 12, the damage state of a rock is presented, which is selected from each of the three water-bearing states. The dry state rock is destroyed after 8 levels of cyclic loading and unloading, and its destruction is in the form of oblique shear destruction, and the number of broken rock pieces after the destruction of the specimen is 3-5 pieces. The natural state rock was destroyed after 6 levels of cyclic loading and unloading, and its damage mode was a combination of oblique shear damage and tensile damage, with the number of crushed rock pieces increasing significantly compared with that of the dry state rock. The water-saturated state rock is destroyed after 5 levels of cyclic loading and unloading, whose damage mode is mainly tensile and accompanied by shear damage, with more rock fragments and more fragmentation after the damage of the specimen.

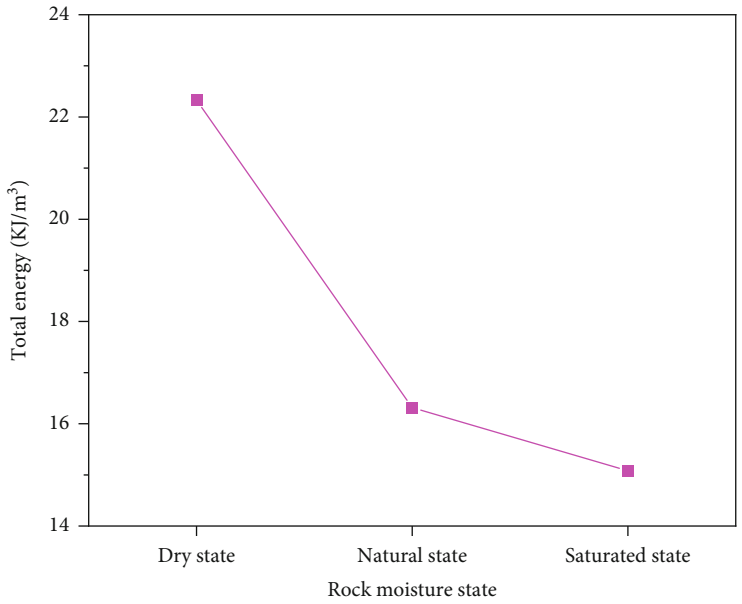

(a) Relationship between water content and total energy

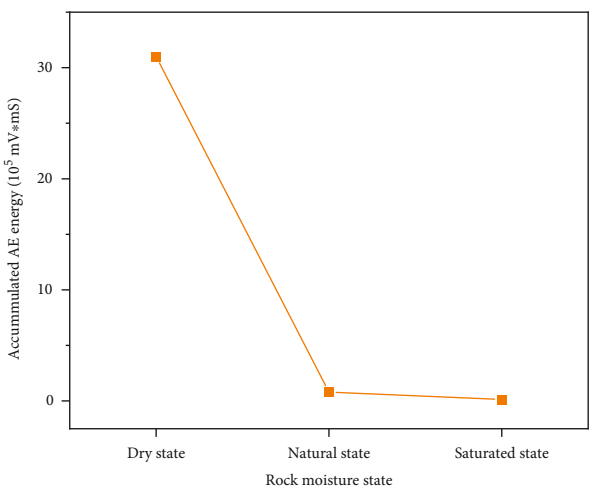

(b) Relationship between water content and accumulated AE energy

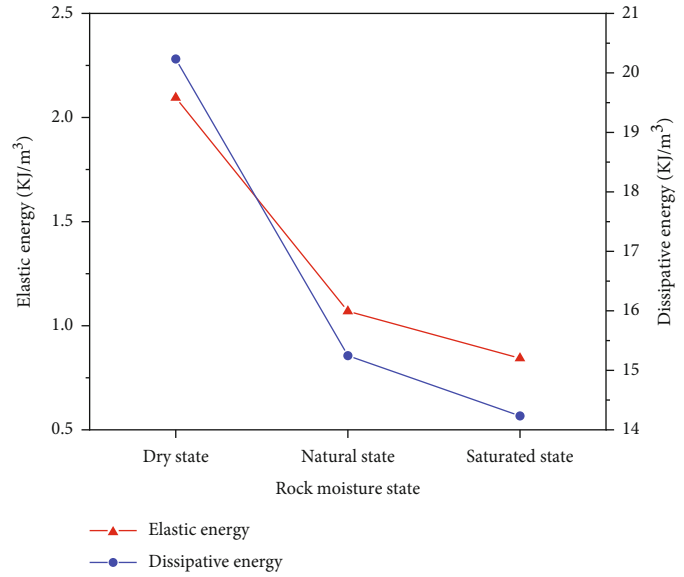

(c) Relationship between water content and elastic energy and dissipation energy

Figure 10: Relationship between water content and each energy change.

Based on the damage patterns of rocks with different water contents, it can be seen that moisture exacerbates fracture extension and complicates the damage patterns, thus affecting the destructive behavior of rocks under impact.

5. Effect of Water Content on Rock Impact Propensity

Rock impact propensity is the natural property of whether coal and rock body can occur impact ground pressure. Coal rock impact propensity is an important basis for evaluating the risk of occurrence of impact ground pressure in coal mines.

The full stress-strain curve of rocks can reflect the mechanical properties of rocks, and it can also visually and comprehensively reflect the whole process of rocks from storing energy to dissipating energy, which contains rich information about impact propensity and is of great significance for revealing the physical nature of impact propensity and analyzing other impact propensity indicators [19].

The impact energy index W_{CF} and the elastic energy index W_{ET} are both indicators for evaluating the impact propensity of rocks. The uniaxial compression test has no energy loss until peak strength is reached, while the impact energy index W_{CF} is the ratio of the elastic strain energy stored in the rock specimen before peak strength to the energy to be consumed in the process after peak strength until complete destruction, which also does not take into account the energy consumed by plastic deformation of coal rock before destruction. The

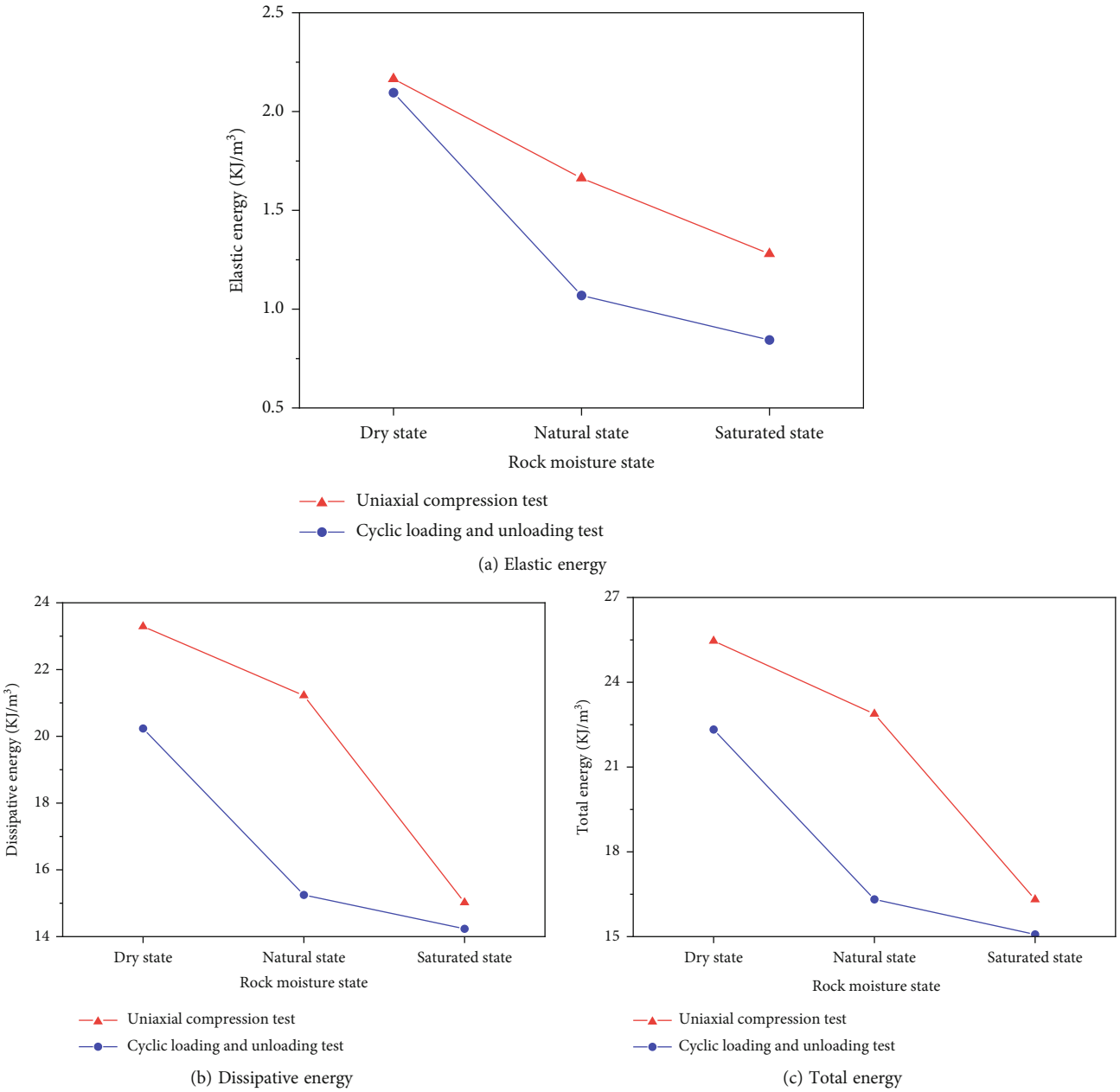

Figure 11: The relationship between each energy of the uniaxial compression test and the cyclic loading and unloading test.

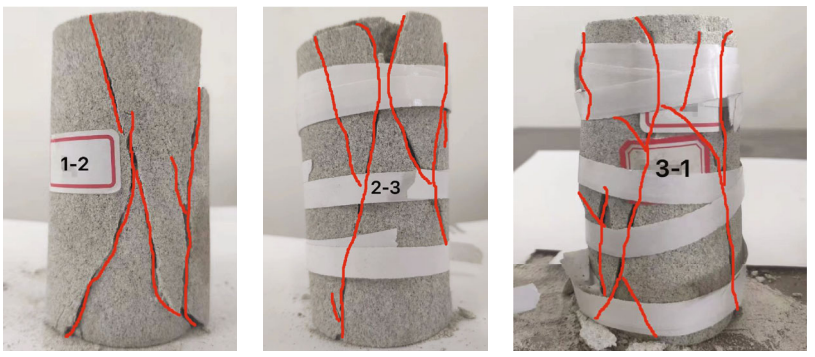

(a) Dry state (b) Natural state (c) Saturation state

Figure 12: Damage states of rocks with different water contents.

Table 3: Schematic values for E_1, E_2, E_E, and E_P.

Rock sample state	Experimental conditions	E_1	E_2	Experimental conditions	E_E	E_P
Dry state		20.75	3.71		11.62	5.88
Natural state	Uniaxial compression	17.009	3.65	Cyclic loading and unloading	7.53	3.82
Saturation state		12.75	3.19		5.84	3.72

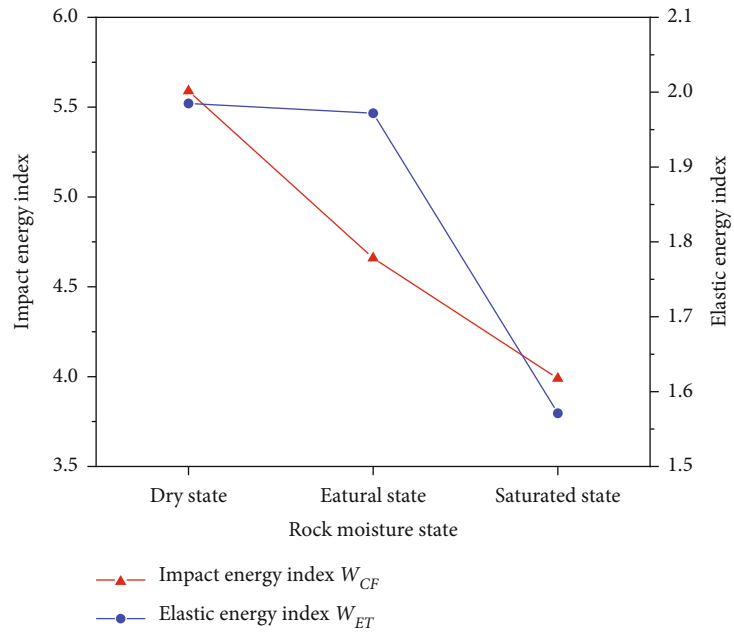

Figure 13: Relationship between water content and W_{CF} and W_{ET}.

elastic energy index W_{ET} is the ratio of the elastic energy accumulated before the destruction of the rock to the energy consumed to produce plastic deformation, which reflects the ability of the coal rock sample to accumulate elastic energy before the peak strength. During the whole process of deformation damage of the rock, the less the elastic strain energy stored in the rock, the more the permanent deformation dissipation energy of the rock and the less the impact tendency of the rock.

$$W_{CF} = \frac{E_1}{E_2}, \tag{9}$$

where E_1 is the elastic strain energy stored before the peak strength and E_2 is the energy to be dissipated in the process after the peak strength until complete destruction.

$$W_{ET} = \frac{E_E}{E_P}, \tag{10}$$

where E_E is the elastic energy accumulated before the destruction of the rock and E_P is the energy consumed by the rock to produce plastic deformation.

Based on the test results and the related equations, the specific values of the components E_1, E_2, E_E, and E_P can be calculated as shown in Table 3.

From the test result parameters, it can be calculated that the impact energy index W_{CF} of the dry state rock is 5.59, and the elastic energy index W_{ET} is 1.985. The impact energy index W_{CF} of the natural state rock is 4.66, and the elastic energy index W_{ET} is 1.972; the impact energy index W_{CF} is 3.99, and the elastic energy index W_{ET} is 1.571 for the saturated state rock. The impact energy index W_{CF} decreased by 28.6%, and the elastic energy index W_{ET} decreased by 20.9% compared with the dry state rock in the saturated state condition. Therefore, with higher water content of the rock, the impact energy index W_{CF} and elastic energy index W_{ET} are smaller.

Table 4: Rock blast tendency indicator values [20].

Impact energy index	Elastic energy index	Rock explosion level
$W_{CF} \le 2$	$W_{ET} \le 2$	No rock burst
$2 \le W_{CF} \le 3$	$2 \le W_{ET} \le 3$	Weak rock burst
$3 \le W_{CF} \le 5$	$3 \le W_{ET} \le 5$	Moderate rock burst
$W_{CF} \ge 5$	$W_{ET} \ge 5$	Strong rock burst

The impact energy index W_{CF} shows the relationship between the magnitude of the elastic energy stored in the rock before damage and the energy dissipated during damage, and the elastic energy index W_{ET} shows the ability of the rock to accumulate elastic energy before damage. As shown in Figure 13, in the case of higher water content of the rock, the impact energy index W_{CF} and elastic energy index W_{ET} are smaller, indicating that the less elastic energy is stored in the rock preliminarily and no excess energy is

transformed into energy in rock crushing when the rock breaks. Combined with Table 4, it can be concluded that with smaller impact energy index$W_{CF}$and elastic energy indexW_{ET}, the rock burst grade of the rock is weaker; that is, the rock impact propensity is smaller.

6. Conclusions

In this paper, uniaxial compression tests, cyclic loading and unloading tests, and acoustic emission tests were conducted on white sandstone specimens with different water-bearing states and analyzed the laws of water content on rock strength characteristics, energy characteristics, and rock impact propensity, and the following conclusions were obtained:

(1) Water has a certain softening effect on rock. The higher the water content of the rock, the more easily the internal structure is softened. The cohesive effect within the rock begins to weaken, which in turn reduces the stiffness of the material, and the plastic becomes stronger. The ability of the rock to resist elastic deformation is poorer, resulting in lower compressive strength and elastic modulus when the rock is subjected to external forces, making it more prone to deformation and damage. The decrease in compressive strength of the saturated state rock is 33.3%, and the decrease in elastic modulus is 28.1% compared to the dry state rock. Compared with the uniaxial compression test, in the loading and unloading cyclic test, the decreases of compressive strength of rocks in the three water content states were 31.8%, 44.2%, and 28.2%, and the decreases of elastic modulus were 6.4%, 15.9%, and 17.8%, respectively

(2) Water content has a significant effect on the energy characteristics of the rock. As the water content increases, the cohesion of the rock decreases and the internal structure of the rock is more easily destroyed, which ultimately makes the energy reached during needed for rock destruction lower. As a result, the total energy, elastic energy, and dissipative energy of the rock are reduced. The accumulated AE energy also decreases with increasing water content of the rock, indicating that rocks with higher water content gather less elastic energy before damage and reach less energy when deformation damage occurs. Before the dramatic change in energy, elastic energy accounts for a larger proportion of the total energy, and energy is dominated by elastic energy, which is expressed as energy aggregation. After the dramatic change in energy, dissipative energy accounts for a larger proportion of the total energy, and energy is dominated by dissipative energy, which is expressed as energy dissipation. Due to the energy loss in the process of loading and unloading of the rock in the loading and unloading cycle test, compared with the uniaxial compression test, the decreases of elastic energy of the rock in the three water content states were 3.21%, 35.70%, and 34.06%; the decreases of dissipated energy were 13.12%, 28.14%, and 5.23%; and the decreases of total energy were 12.84%, 28.68%, and 7.55%, respectively

(3) The impact energy index W_{CF} and elastic energy index W_{ET} are negatively correlated with the water content. Both the elastic energy index W_{ET} and impact energy index W_{CF} decrease with increasing water content of the rock. The impact energy index W_{CF} is reduced by 28.6%, and the elastic energy index W_{ET} is reduced by 20.9% for the saturated rock compared to the dry rock. The smaller the impact energy index W_{CF} and the elastic energy index W_{ET}, the less elastic energy is stored in the rock beforehand, and there is no excess energy transformed into the energy of rock crushing when the rock is destroyed, so the rock impact tendency is smaller.

Data Availability

The data used to support the findings of this study are available from the corresponding author upon request.

Conflicts of Interest

The authors declare that they have no conflicts of interest.

Acknowledgments

This research was supported by the Anhui Provincial Natural Science Foundation (2008085ME147) and the National Natural Science Foundation of China (52174103).

References

[1] W.-h. Zheng, T.-w. Shi, and Y.-S. Pan, "Study on the effect of water content on the charge induction signal of rocks," *Geotechnics*, vol. 43, no. 3, p. 10, 2022.

[2] X.-b. Mao, L.-y. Zhang, and R.-x. Liu, "Uniaxial creep properties and damage intrinsic relationship of mudstone under high temperature," *Journal of Geotechnical Engineering*, vol. 35, no. 2, pp. 30–37, 2013.

[3] Z.-y. Tao, "Rock bursts in high ground stress areas and their discrimination," *People's Changjiang*, vol. 4, no. 5, pp. 25–32, 1987.

[4] S. Cheng-dong, X.-x. Zhai, and Z.-x. Wei, "Influence of water saturation time on the impact propensity index of 2# coal seam in Qianqiu coal mine," *Journal of Rock Mechanics and Engineering*, vol. 33, no. 2, pp. 235–242.

[5] F. Xiao-min, "Experimental study on uniaxial compression deformation and acoustic emission characteristics of typical rocks," *Journal of Chengdu University of Technology: Natural Science Edition*, vol. 32, no. 1, p. 5, 2005.

[6] F.-j. Yang, H. Zhou, and J.-j. Lu, "Energy discrimination index of rock explosion process," *Journal of Rock Mechanics and Engineering*, vol. 34, no. S1, pp. 2706–2714, 2015.

[7] P. Chao, L.-b. Meng, and T.-b. Li, "Study on fracture and energy characteristics of kilomorphic rocks under triaxial compression conditions," *Journal of Engineering Geology*, vol. 25, no. 2, pp. 359–366, 2017.

[8] D. G. Roy, T. N. Singh, and J. Kodikara, "Effect of water saturation on the fracture and mechanical properties of sedimentary rocks," *Rock Mechanics and Rock Engineering*, vol. 50, no. 10, pp. 2585–2600, 2017.

[9] D. P. Jansen, S. R. Carlson, and R. P. Young, "Ultrasonic imaging and acoustic emission monitoring of thermally induced microcracks in Lacdu Bonnet granite," *Journal of Geophysical Research*, vol. 98, no. 12, pp. 2231–2243, 1993.

[10] The Professional Standards Compilation Group of People's Republic of China, *DL T 5368 — 2007 Code for Rock Tests of Hydroelectric and Water Conservanty Engineering*, China Electric Power Press, Beijing, 2007.

[11] C.-m. Li, N. Liu, W.-r. Liu, and R. Feng, "Study on characteristics of energy storage and acoustic emission of rock under different moisture content," *Sustainability*, vol. 13, no. 3, p. 1041, 2021.

[12] H.-l. Jia, T. Wang, W. Xiang, L. Tan, Y.-j. Shen, and G.-s. Yang, "Laws and mechanisms of the effect of water content on the physical and mechanical properties of muddy siltstones," *Journal of Rock Mechanics and Engineering*, vol. 37, no. 7, pp. 1618–1628, 2018.

[13] H.-p. Xie and Z.-h. Chen, "Rock mechanics," Science Press, Beijing, 2004.

[14] H.-p. Xie, J. Yang, and L.-y. Li, "Rock strength and integral damage criterion based on energy dissipation and release principle," *Journal of Rock Mechanics and Engineering*, vol. 24, no. 17, pp. 3003–3010, 2005.

[15] X.-f. Liu and Y.-g. Wang, "Investigation into law of AE energy accumulation and damage evolution on coal and rock," *Journal of Liaoning University of Engineering and Technology: Natural Science Edition*, vol. 30, no. 1, 2011.

[16] T.-b. Li, Z.-q. Chen, G.-q. Chen, C.-c. Ma, O.-l. Tang, and M.-j. Wang, "Study on the energy mechanism of sandstone under the action of different water content," *Geotechnics*, vol. 36, no. S2, pp. 229–236, 2015.

[17] Z.-x. Liu, W. Wang, J.-a. Luo, and G.-h. Miao, "Energy evolution analysis method in rock uniaxial compression test," *Journal of Coal*, vol. 45, no. 9, p. 9, 2020.

[18] J.-f. Jin, X. Yu, and Y.-l. Zhong, "Characteristics of energy dissipation during impact in red sandstones with different water contents," *Non-Ferrous Metal Science and Engineering*, vol. 12, no. 5, 2021.

[19] H.-t. Wang, J. Xu, F.-s. Wei, and X.-f. Xian, *Evaluation of Impact Propensity Index of Coal Rock Body*, Mine pressure and roof management, 1999.

[20] MT/T 174-2000, *Classification and Laboratory Test Method on Bursting Liability of Coal*Industry Standards - Coal.